Radio Channel Modelling Using Stochastic Propagation Graphs

Pedersen, Troels; Fleury, Bernard Henri

Published in:
IEEE International Conference on Communications. ICC'07

DOI (link to publication from Publisher):
10.1109/ICC.2007.454

Publication date:
2007

Document Version
Publisher's PDF, also known as Version of record

This full text paper was peer reviewed at the direction of IEEE Communications Society subject matter experts for publication in the ICC 2007 proceedings.

Radio Channel Modelling Using Stochastic Propagation Graphs

Troels Pedersen and Bernard H. Fleury
Department of Electronic Systems, Aalborg University,
DK-9220 Aalborg East, Denmark. Email: {troels,fleury}@es.aau.dk

Abstract— **In this contribution the radio channel model proposed in [1] is extended to include multiple transmitters and receivers. The propagation environment is modelled using random graphs where vertices of a graph represent scatterers and edges model the wave propagation between scatterers. Furthermore, we develop a closed form analytical expression for the transfer matrix of the propagation graph. It is shown by simulation that impulse response and the delay-power spectrum of the graph exhibit exponentially decaying power as a result of the recursive scattering structure of the graph. The impulse response exhibits a transition from specular to diffuse signal contributions as observed in measurements.**

I. Introduction

The design and optimisation of modern radio communication systems require realistic models of the radio propagation channel, which incorporate dispersion in delay, Doppler frequency, direction of departure, direction of arrival, and polarisation. Often radio communication systems are assessed by Monte Carlo simulations in which stochastic models are used to generate synthetic realisations of the response of the (radio) propagation channel.

Traditional stochastic radio channel models reflect the statistical properties of the (time-variant or time-invariant) impulse response of the channel between the input of any antenna element at the transmitter site and the output of any antenna element at the receiver site. The probability distributions of the parameters of the channel impulse response are generally difficult to obtain from environment parameters such as the scatterer size and density. Instead, the model parameters are often inferred from measurements. Motivated by experimental results, conventional models implement an exponentially decaying delay-power spectrum and impulse response magnitude by including various ad-hoc constraints on the random model parameters. The two contributions [2] and [3] follow this approach. In these models a key parameter for modelling the arrival times of individual signal components is the "cluster arrival rate". However this parameter is difficult to derive from a propagation environment. In the model given in [4] the scattering coefficients are corrected to account for the effects observed experimentally like the exponential decay of the delay-power spectrum. These approaches, however, do not reflect the underlying physical mechanisms that lead to this decaying behaviour.

A different approach is followed by Franceschetti in [5] where the radio propagation mechanism is modelled as a "stream of photons" performing a continuous random walk in a cluttered environment with constant clutter density. The transmitted signal is a pulse of finite duration. When a photon interacts with an obstacle, it is either absorbed (with a certain probability) or scattered and changes direction. The Franceschetti model is mainly a descriptive model for the delay-power spectrum; it is not possible to obtain realistic realisations of the channel impulse responses from this model. Furthermore, the model does not cover the transition from specular to diffuse signal contributions as observed in [6] for ultra wide band measurements. This transition effect is well-known within the field of room acoustics [7]. In a recently published work [8] Andersen *et. al* model the exponentially decaying power of the diffuse tail of the impulse response by applying Sabine's reverberation formula commonly used in room acoustics. In the work presented in [1] the propagation environment was modelled using random graphs where vertices of a graph represent scatterers and edges model the wave propagation between scatterers. When a graph is generated, the corresponding realisation of the channel impulse response can be computed by exhaustively searching for propagation paths that connect the transmitter to the receiver. The obtained impulse response exhibits the specular-to-diffuse transition.

In this contribution we extend the model described in [1] to include multiple transmitters and receivers. We develop a closed form analytical expression for the transfer matrix. The derivation is inspired from the method used in the room acoustical model proposed in [9].

The remaining part of the paper is organised as follows. In Section II the modelling concept based directed graphs is presented and a model of the propagation environment is introduced. In Section III an analytical expression for the transfer matrix of the propagation graph is derived. Numerical examples are given in Section IV and concluding remarks are addressed in Section V.

II. Modelling Propagation Using Graphs

In the following we describe the underlying principles for modelling the propagation mechanisms using graphs. In a typical propagation scenario, the electromagnetic signal emitted by a transmitter propagates through the environment interacting with a number of objects called scatterers. The receiver, which is usually placed away from the transmitter, picks up the transmitted signal. If a line-of-sight exists between the transmitter and receiver, direct propagation occurs. In other cases, indirect propagation via one ore more scatterers can

1-4244-0353-7/07/$25.00 ©2007 IEEE

occur. In the following we represent the propagation environment as a directed graph where the vertices represent the transmitters, receivers, and scatterers, and the edges represent visibilities between the vertices. First, the necessary notation is introduced.

A. Directed Graphs

Following [10] we define a directed graph $\mathcal{G}$ as a pair $(\mathcal{V}, \mathcal{E})$ of disjoint sets (of vertices and edges) together with the two mappings $\mathrm{init} : \mathcal{E} \to \mathcal{V}$ and $\mathrm{term} : \mathcal{E} \to \mathcal{V}$ assigning every edge $e \in \mathcal{E}$ an initial vertex $\mathrm{init}(e)$ and a terminal vertex $\mathrm{term}(e)$.

Two edges e and e' are parallel if $\mathrm{init}(e) = \mathrm{init}(e')$ and $\mathrm{term}(e) = \mathrm{term}(e')$. When the discussion is restricted to graphs without parallel edges we may identify the edge e with $(\mathrm{init}(e), \mathrm{term}(e)) \in \mathcal{V}^2$ and write $e = (\mathrm{init}(e), \mathrm{term}(e))$ with a slight abuse of notation. With this identification, $\mathcal{E} \subseteq \mathcal{V}^2$.

A walk (of length K) in a graph $\mathcal{G}$ is a non-empty alternating sequence $\langle v_1, e_1, v_2, e_2, \ldots, e_K, v_{K+1} \rangle$ of vertices and edges in $\mathcal{G}$ such that $\mathrm{init}(e_k) = v_k$ and $\mathrm{term}(e_k) = v_{k+1}$, $1 \leq k < K$. An edge $e \in \mathcal{E}$ that fulfils $\mathrm{init}(e) = \mathrm{term}(e)$ is called a loop. Thus, by definition, a loop is a walk of length 1. A path is a walk, without parallel edges, where the vertices $v_2, \ldots, v_{K-1}$ are distinct. A path that fulfils $v_1 = v_K$ is called a cycle. The outdegree of a vertex v denoted by $\deg_i(v)$ is the number of edges with initial vertex v.

B. Propagation Graphs

A propagation graph is a directed graph $\mathcal{G} = (\mathcal{V}, \mathcal{E})$ where the vertices model transmitters, receivers and scatterers, and the edges model the propagation conditions between the vertices.

The vertex set of a propagation graph is a union of three disjoint sets: $\mathcal{V} = \mathcal{V}_\mathrm{t} \cup \mathcal{V}_\mathrm{s} \cup \mathcal{V}_\mathrm{r}$, where $\mathcal{V}_\mathrm{t} = \{\mathrm{Tx}1, \ldots, \mathrm{Tx}M_1\}$ is the set of transmit vertices, $\mathcal{V}_\mathrm{r} = \{\mathrm{Rx}1, \ldots, \mathrm{Rx}M_2\}$ the set of receive vertices, and $\mathcal{V}_\mathrm{s} = \{\mathrm{S}1, \ldots, \mathrm{S}N\}$ is the set of scatterer vertices. Fig. 1 shows a propagation graph for a communication system with $M_1 = 5$ transmitters, $M_2 = 3$ receivers, and $N = 6$ scatterers. The depicted graph has one cycle. Each vertex $v \in \mathcal{V}$ is assigned a coordinate in space with respect to a coordinate system and arbitrarily selected origin. The vector $\mathbf{r}_v \in \mathcal{R} \subseteq \mathbb{R}^3$, denotes the displacement vector of v from the origin of the coordinate system. The set $\mathcal{R}$ is the region in which contains the scatterers that significantly affect the propagation mechanisms between the transmitters and a receivers in the graph.

In the case depicted in Fig. 1, all transmit vertices are located in the close proximity of each other, away from the other vertices which is also the case for the receive vertices. This corresponds to the case where the transmitter and receiver sites are equipped with antenna arrays. This is not the case in multi-user systems, where the transmitters and receivers are spread evenly in space.

The edges of a propagation graph model the propagation, or the visibility, between vertices meaning that a signal emitted from the initial vertex is observed in a filtered (e.g. delayed and attenuated) version at the terminal vertex. Due to this conceptual interpretation of an edge, a propagation graph does not have parallel edges. In this case we may identify the edge e with $(\mathrm{init}(e), \mathrm{term}(e)) \in \mathcal{V}^2$ and write $e = (\mathrm{init}(e), \mathrm{term}(e))$ with a slight abuse of notation. With this identification, $\mathcal{E} \subseteq \mathcal{V}^2$. Notice that $\mathcal{G}$ may have "anti-parallel" edges, i.e. if the edge $e = (v, v')$ is in the graph, the edge $e' = (v', v)$ can exist. We restrict the discussion to propagation graphs where scatterers cannot "see" themselves. Hence we only deal with graphs without loops. However, the propagation graphs may have cycles. The transmit vertices are considered as purely sources with outgoing edges. Likewise, the receivers are considered as sinks with only incoming edges.

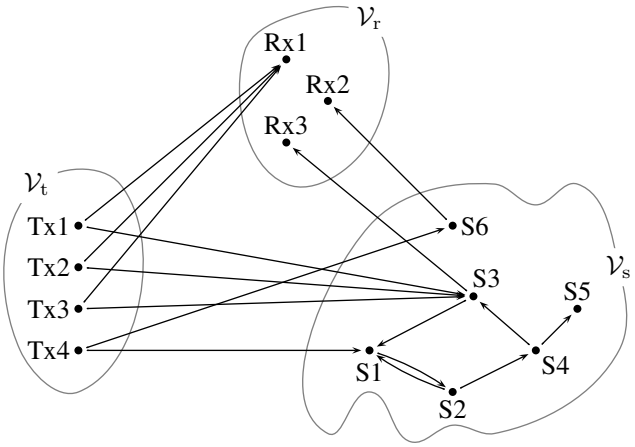

Fig. 1. A propagation graph with four transmit vertices ($M_1 = 4$), three receive vertices ($M_2 = 3$), and six scatterer vertices ($N = 6$).

The signal propagates in the graph in the following way. Each transmitter emits a signal that propagate via the edges of the graph. The signals observed by a receiver vertex is the sum of the signals arriving via the incoming edges. The scatterers sum up the signals arriving via the incoming edges and re-emit the sum-signals via the outgoing edges. When a signal propagates along an edge, or interacts with a scatterer, the signal undergoes dispersion in time, depending on the length of the edge and the particular scattering mechanisms. The joint mechanism of propagating along an edge and interaction with a scatterer is assumed linear, thus the time dispersion of the signal can be represented as a convolution with an impulse response or, in the Fourier domain, as a multiplication with a transfer function.

C. Model of the Propagation Mechanisms

In the following we discuss a model where the propagation along the edges is assumed to be non-dispersive in delay in the sense that the impulse response of each edge is merely a scaled and delayed Dirac impulse. Let g_e and τ_e denote respectively the complex gain and propagation time of edge e. Thus the edge transfer functions $A_e(f)$ takes the form

$$A_e(f) = g_e \cdot \exp(j2\pi\tau_e f), \quad e \in \mathcal{E}. \tag{1}$$

The complex gain g_e includes the gain due to the propagation loss along edge e and the scattering coefficient due to the interaction at $\mathrm{term}(e)$. This scatterer model is suitable in situations where the electromagnetic properties of the scatterers are constant over the bandwidth of the transmitted signal. In the sequel a method for determining the edge gains and attenuations is described.

The propagation time τ_e of a signal propagating along edge $e = (v, v')$ in $\mathcal{E}$ can be calculated from the coordinates of v and v' as

$$\tau_e = \frac{|\mathbf{r}_v - \mathbf{r}_{v'}|}{c}, \tag{2}$$

where $c \approx 3 \cdot 10^8\,\mathrm{m/s}$ is the speed of light (in vacuum) and $|\cdot|$ is the Euclidean norm. The power gain $|g_e|^2$ of $e \in \mathcal{E}$ is defined as

$$|g_e|^2 = \left(\frac{g}{1 + |\mathbf{r}_v - \mathbf{r}_{v'}|}\right)^2 \cdot \tfrac{1}{\deg_o(v)}. \tag{3}$$

For large edge lengths $|\mathbf{r}_v - \mathbf{r}_{v'}|$, (3) behaves like the standard inverse squared distance power law. Notice that since $\deg_o(v) = 0$ if and only if $e \notin \mathcal{E}$, and the term $1+|\mathbf{r}_v - \mathbf{r}_{v'}| \geq 1$, the gain $|g_e|^2$ is finite for all $e \in \mathcal{V}^2$. The definition (3) ensures that the power leaving a vertex is always smaller than the power entering the vertex. The phase of g_e can be chosen according to some appropriate model. As an example, when a multiuser systems is modelled, this phase can be assumed to be uniformly distributed on the interval $[0; 2\pi)$. However, if the transmitters and receivers forms arrays, then more careful modelling of the phases is necessary.

D. Modelling Systems With Antenna Arrays

Considering a system where the transmit antennas are spatially grouped such that they form an array, it is customary to make the so-called 'small-scale characterisation'. This assumption states that the overall geometry of each propagation path is the same for all antenna elements of one antenna array. This corresponds to a propagation graph where all elements of an array share the same visibilities. We can distinguish 'small' and 'large' arrays as follows:

An array $\mathcal{A} \subseteq \mathcal{V}_\mathrm{t}$ of transmit vertices is a *small array*, if, and only if, for any edge $e = (v, v')$ from a transmitter vertex $v \in \mathcal{A}$ to a receiver or scatterer vertex $v' \in \mathcal{V}_\mathrm{s} \cup \mathcal{V}_\mathrm{r}$ the set of edges $\{(v'', v') : \ v'' \in \mathcal{A}\}$ is a subset of $\mathcal{E}$. If an array is not small then it is a *large array*. The generalisation of the definition to include receive antennas is obvious.

In the situation depicted in Fig 1, the transmit antennas $\mathrm{Tx1}, \mathrm{Tx2}, \mathrm{Tx3}$ and $\mathrm{Tx4}$ form an array $\mathcal{A} = \{\mathrm{Tx1}, \mathrm{Tx2}, \mathrm{Tx3}, \mathrm{Tx4}\}$. As can be seen from the figure, edge $(\mathrm{Tx1}, \mathrm{Rx1})$ exists. Since there is not an edge $(\mathrm{Tx4}, \mathrm{Rx1})$ in the graph, the array $\mathcal{A}$ is a large array. It can be checked that the sub-array $\{\mathrm{Tx1}, \mathrm{Tx2}, \mathrm{Tx3}\}$ form a small array.

It should be noticed that not all practical arrays are small (see [11] for an example). However, by applying appropriate restrictions on the edge-set of the graph, the propagation graphs can be used to model both small and large arrays. For a small array $\mathcal{A}$, it seems to be natural to assume that the edge gains of the set of edges which connects the elements of $\mathcal{A}$ to a particular vertex $v \notin \mathcal{A}$ all have the same phase.

III. The Transfer Matrix of a Propagation Graph

In the following we derive the input-output relation of a propagation graph. By the definition of the propagation graph, there are no other signal sources than the vertices in $\mathcal{V}_\mathrm{t}$. Thus by assuming that the propagation mechanisms are linear and time-invariant, the Fourier domain version of the input-output relation can be written as

$$\mathbf{Y}(f) = \mathbf{H}(f)\mathbf{X}(f), \tag{4}$$

where $\mathbf{H}(f)$ is $M_2 \times M_1$ transfer matrix. The M_1-dimensional input signal $\mathbf{X}(f)$ is defined as

$$\mathbf{X}(f) = [X_1(f), \ldots, X_{M_1}(f)]^\mathrm{t}, \tag{5}$$

where $X_m(f)$ is the signal emitted by transmitter $\mathrm{Tx}m$, and $[\,\cdot\,]^\mathrm{t}$ denotes the transposition operator. The output signal vector $\mathbf{Y}(f)$ is defined as

$$\mathbf{Y}(f) = [Y_1(f), \ldots, Y_{M_2}(f)]^\mathrm{t}, \tag{6}$$

where $Y_m(f)$ is the Fourier transform of the signal observed by receiver $\mathrm{Rx}m$.

Similar, to $\mathbf{X}(f)$ and $\mathbf{Y}(f)$ we can define a vector $\mathbf{Z}(f)$ to describe the signal observed at the scatterers as

$$\mathbf{Z}(f) = [Z_1(f), \ldots, Z_N(f)]^\mathrm{t}, \tag{7}$$

where the nth entry denotes the Fourier transform of the signal observed at scatterer vertex $\mathrm{S}n$.

We form the M_1+M_2+N dimensional complex state vector $\mathbf{C}(f)$ as

$$\mathbf{C}(f) = [C_1(f), \ldots, C_n(f), \ldots C_{M_1+M_2+N}(f)]^\mathrm{t}, \tag{8}$$

where $C_n(f)$ is the state variable of vertex v_n. By selecting the indexing of the vertices according to

$$v_n \in \begin{cases} \mathcal{V}_\mathrm{t}, & n = 1, \ldots, M_1 \\ \mathcal{V}_\mathrm{r}, & n = M_1 + 1, \ldots, M_1 + M_2 \\ \mathcal{V}_\mathrm{s}, & n = M_1 + M_2 + 1, \ldots, M_1 + M_2 + N, \end{cases} \tag{9}$$

it is seen that

$$\mathbf{C}(f) = [\mathbf{X}(f)^\mathrm{t}, \mathbf{Y}(f)^\mathrm{t}, \mathbf{Z}(f)^\mathrm{t}]^\mathrm{t}. \tag{10}$$

Let us for a moment consider the edge $e = (v_n, v_{n'})$ in $\mathcal{E}$. A filtered version of the signal $C_n(f)$ emitted by vertex v_n is observed at vertex $v_{n'}$. The signal observed at vertex $v_{n'}$ via edge e reads $A_e(f)C_n(f)$ where $A_e(f)$ is the edge transfer function defined in (1). In other words, the transfer function $A_e(f)$ describes the propagation along the edge e, i.e. the propagation delay, attenuation, and the scattering coefficient at the initial vertex of e. By collecting the edge transfer functions to a matrix using the indexing described in (9) we obtain the weighted adjacency matrix

$\mathbf{A}(f) \in \mathbb{C}^{(M_1+M_2+N)\times(M_1+M_2+N)}$ of the entire propagation graph $\mathcal{G}$:

$$[\mathbf{A}(f)]_{nn'} = \begin{cases} A_{(v_n,v_{n'})}(f) & \text{if } (v_n, v_{n'}) \in \mathcal{E}, \\ 0 & \text{otherwise.} \end{cases} \tag{11}$$

Element n, n' of $\mathbf{A}(f)$ is the transfer function from vertex v_n to vertex $v_{n'}$ of $\mathcal{G}$. Due to the selected vertex indexing the weighted adjacency matrix can be partitioned as

$$\mathbf{A}(f) = \begin{bmatrix} \mathbf{0} & \mathbf{0} & \mathbf{0} \\ \mathbf{D}(f) & \mathbf{0} & \mathbf{R}(f) \\ \mathbf{T}(f) & \mathbf{0} & \mathbf{B}(f) \end{bmatrix}, \tag{12}$$

where $\mathbf{0}$ denotes a zero matrix of the appropriate dimension and

$$\mathbf{D}(f) \in \mathbb{C}^{M_2\times M_1} \quad \text{connects transmitters to receivers} \tag{13}$$
$$\mathbf{R}(f) \in \mathbb{C}^{M_2\times N} \quad \text{connects scatterers to receivers} \tag{14}$$
$$\mathbf{T}(f) \in \mathbb{C}^{N\times M_1} \quad \text{connects transmitters to scatterers} \tag{15}$$
$$\mathbf{B}(f) \in \mathbb{C}^{N\times N} \quad \text{interconnects the scatterers.} \tag{16}$$

The special structure of $\mathbf{A}(f)$ origins from the structure of the propagation graph. The first M_1 rows are zero because, we do not accept incoming edges into the transmitters. Likewise column $M_1 + 1, \ldots, M_1 + M_2$ are all zero since the receiver vertices have no outgoing edges. Furthermore, since the propagation graph contains no loops the entries of the main diagonal of the adjacency matrix $\mathbf{A}(f)$ are zero. Therefore the entries of the main diagonal of $\mathbf{B}(f)$ are zero.

The state vector $\mathbf{C}(f)$ can be rewritten as the sum

$$\mathbf{C}(f) = \sum_{k=0}^{\infty} \mathbf{C}_k(f), \tag{17}$$

where $\mathbf{C}_k(f) = [\mathbf{X}_k(f)^{\mathrm{t}}, \mathbf{Y}_k(f)^{\mathrm{t}}, \mathbf{Z}_k(f)^{\mathrm{t}}]^{\mathrm{t}}$ denotes the signal contribution that has propagated along k edges. The signal emitted by the transmitters has not propagated via any edges and therefore $\mathbf{X}_0(f) = \mathbf{X}(f)$. For $k = 0$ we have

$$\mathbf{C}_0(f) = [\mathbf{X}(f)^{\mathrm{t}}, \mathbf{0}^{\mathrm{t}}, \mathbf{0}^{\mathrm{t}}]^{\mathrm{t}}, \tag{18}$$

and for $k \geq 1$ we have the recursive relation:

$$\mathbf{C}_{k+1}(f) = \mathbf{A}(f)\mathbf{C}_k(f), \quad k \geq 1. \tag{19}$$

As a consequence of (17), the output signal vector can be decomposed as the sum

$$\mathbf{Y}(f) = \sum_{k=1}^{\infty} \mathbf{Y}_k(f), \tag{20}$$

where $\mathbf{Y}_k(f)$ is the received signal component that has propagated via k edges from the transmitter to the receiver. Thus $\mathbf{Y}_1(f)$ is the component originating from direct propagation from the transmitters to the receivers. By direct computation of $\mathbf{C}_1(f)$ using (19) and (18) we see that

$$\mathbf{C}_1(f) = \mathbf{A}(f)\mathbf{C}_0(f) = \begin{bmatrix} \mathbf{0} \\ \mathbf{D}(f)\mathbf{X}(f) \\ \mathbf{T}(f)\mathbf{X}(f) \end{bmatrix}. \tag{21}$$

It follows from (21) that

$$\mathbf{Y}_1(f) = \mathbf{D}(f)\mathbf{X}(f). \tag{22}$$

By inspection of the series $\mathbf{A}^2(f), \mathbf{A}^3(f), \ldots$ it is readily recognised that

$$\mathbf{A}^k(f) = \begin{bmatrix} \mathbf{0} & \mathbf{0} & \mathbf{0} \\ \mathbf{R}(f)\mathbf{B}^{k-2}(f)\mathbf{T}(f) & \mathbf{0} & \mathbf{R}(f)\mathbf{B}^{k-1}(f) \\ \mathbf{B}^{k-1}(f)\mathbf{T}(f) & \mathbf{0} & \mathbf{B}^k(f) \end{bmatrix}, \; k \geq 2. \tag{23}$$

Inserting (22) and (23) into (20) and using (19) yields

$$\mathbf{Y}(f) = \mathbf{Y}_1(f) + \sum_{k=2}^{\infty} \mathbf{Y}_k(f) \tag{24}$$
$$= \mathbf{D}(f)\mathbf{X}(f) + \sum_{k=2}^{\infty} \mathbf{R}(f)\mathbf{B}^{k-2}(f)\mathbf{T}(f)\mathbf{X}(f) \tag{25}$$
$$= \left[\mathbf{D}(f) + \sum_{k'=0}^{\infty} \mathbf{R}(f)\mathbf{B}^{k'}(f)\mathbf{T}(f)\right]\mathbf{X}(f) \tag{26}$$
$$= \underbrace{\left[\mathbf{D}(f) + \mathbf{R}(f)(\mathbf{I} - \mathbf{B}(f))^{-1}\mathbf{T}(f)\right]}_{\mathbf{H}(f)}\mathbf{X}(f). \tag{27}$$

Identity (27) is obtained using geometric series for matrices [12, p. 427], which holds under the condition that the maximum of the eigenvalue magnitudes of $\mathbf{B}(f)$ is less than unity for all frequencies considered. This constraint is always fulfilled for a propagation graph due the definition of the edge gain (3).

Equation (19) shows the structure of the propagation mechanism. The radio signal is re-scattered successively in the propagation environment. This effect results in the geometric series in (26). From (27) we see that the transfer matrix $\mathbf{H}(f)$ consists of the two following terms: $\mathbf{D}(f)$ representing direct propagation between the transmitters and receivers and $\mathbf{R}(f)(\mathbf{I} - \mathbf{B}(f))^{-1}\mathbf{T}(f)$ describing indirect propagation.

IV. Numerical Examples

Using the analytical results from Section III we are able to compute the transfer matrix of a particular propagation graph. The propagation graph is fully defined by the vertex set, the vertex locations, and the edge set of the graph. Thus, a propagation graph can be generated stochastically by randomly placing the vertices and generating the edges set.

In the sequel we investigate the impulse response and the delay-power spectrum of the propagation graph model by means of a Monte-Carlo experiment. The following scenario is assumed:

- The region $\mathcal{R}$ is assumed to be a rectangular solid box.
- To simplify the discussion we consider a single-input single-output ($M_1 = M_2 = 1$) system. The locations of the transmitter and receiver vertices are fixed throughout the experiment.
- The number N of scatterers is assumed constant.
- The positions of the scatterer vertices are drawn according to a uniform distribution defined on $\mathcal{R}$.

TABLE I

PARAMETER SETTING FOR THE SIMULATION

Parameters	Values
$\mathcal{R}$	$[0,5]\times[0,10]\times[0,3.5]\,\mathrm{m}^3$
$\mathbf{r}_{\mathrm{Tx}}$	$[1.8,\ 2.0,\ 0.5]^{\mathrm{T}}\,\mathrm{m}$
$\mathbf{r}_{\mathrm{Rx}}$	$[1.0,\ 4.0,\ 1.0]^{\mathrm{T}}\,\mathrm{m}$
N	20
g	$0.8\ \mathrm{s}^2$
P_{vis}	0.8
Number of Monte Carlo runs	1000
Signal bandwidth $[f_{\min}, f_{\max}]$	$[2,3]\,\mathrm{GHz}$
Δf	$0.5\,\mathrm{MHz}$
IFFT window	Hanning

- We define the occurrence probability $P_{(v,v')}$ of an edge $(v,v')\in\mathcal{V}^2$ as

$$P_{(v,v')}=\begin{cases}P_{\mathrm{dir}} & \text{if } (v,v')=(\mathrm{Tx},\mathrm{Rx})\\ 0 & \text{if } v=v'\\ 0 & \text{if } v'=\mathrm{Tx} \text{ or } v=\mathrm{Rx},\ \text{and}\\ P_{\mathrm{vis}} & \text{otherwise,}\end{cases}$$

  where P_{dir} denotes the probability of the direct propagation between the transmitter and receiver. When $P_{\mathrm{dir}}=0$ the direct term $\mathbf{D}(f)$ in (27) takes the value zero corresponding to a non-line-of-sight scenario. When $P_{\mathrm{dir}}=1$ direct propagation between transmitter and receiver always occurs which corresponds to a line-of-sight scenario. In this case $\mathbf{D}(f)$ is non-zero.

The parameter settings are given in Table I. In each Monte Carlo run the following steps are performed:

1) Generate scatterer positions $\mathbf{r}_v,\ v\in\mathcal{V}_{\mathrm{s}}$.
2) Generate the edge set $\mathcal{E}$.
3) Compute the transfer function $\mathbf{H}(f)$ for the frequencies $f=f_{\min}, f_{\min}+\Delta f,\ldots,f_{\max}$
4) Compute the inverse Fourier transform of the transfer function applying a Hanning window to reduce sidelobes.

An example of an obtained transfer function for $P_{\mathrm{dir}}=0,1$ and corresponding impulse response are reported in Fig. 2. The magnitude of the transfer function for the $P_{\mathrm{dir}}=0$ exhibits fading over the considered frequency band, whereas the function obtained in the $P_{\mathrm{dir}}=1$ case, which is about 10 dB higher, is more constant. The reported impulse responses magnitudes are roughly exponentially decaying. In the reported case, the impulse responses exhibit a concentration of power into "clusters". Inspection of the vertex positions of the particular realisation revealed that this effect is not caused by geometrically clustering of the scatterers but is an effect of the structure of the graph.

An estimate of the delay-power spectrum can be obtained by computing the mean squared-magnitude of the generated impulse response realisations. Estimates of the delay-power spectra for $P_{\mathrm{dir}}=0,1$ each obtained from 1000 realisations of the impulse response are shown in Fig. 3. Apart from the high-magnitude of the direct component in the $P_{\mathrm{dir}}=0,1$, both delay-power spectra in Fig. 3 show similar behaviour:

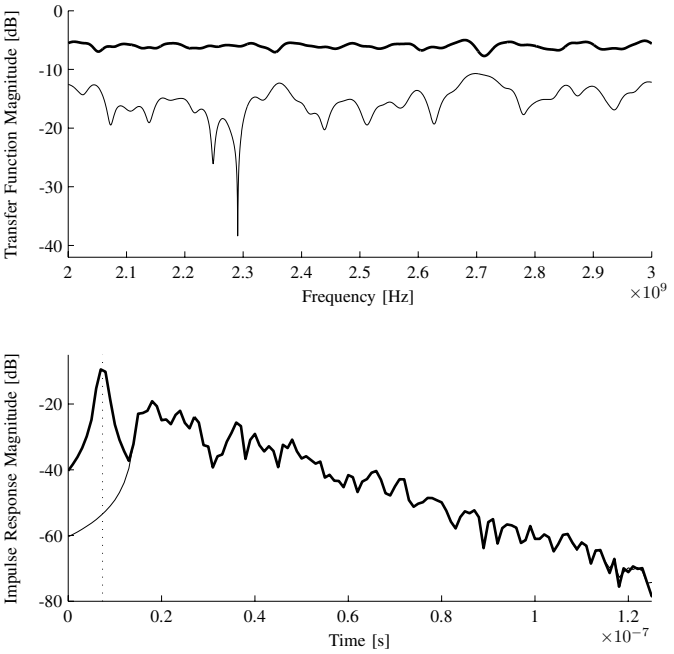

Fig. 2. Examples of transfer functions (top) and the corresponding impulse responses (bottom) for $P_{\mathrm{dir}}=1$ (thick line) and $P_{\mathrm{dir}}=0$ (thin line). The dotted vertical line marks the propagation delay of the direct edge between the transmitter and the receiver (line-of-sight). The parameter setting used in the simulations is listed in Table I.

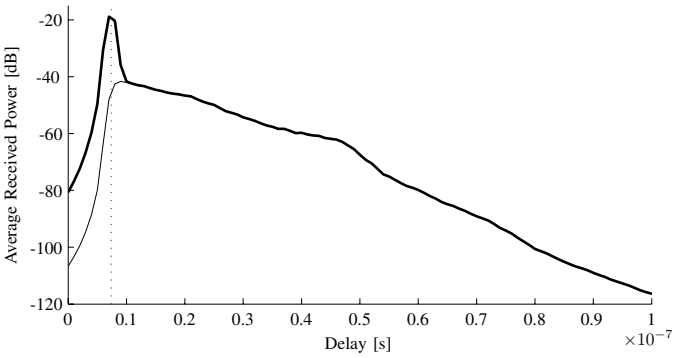

Fig. 3. Delay-power spectrum computed from the Monte Carlo experiment for $P_{\mathrm{dir}}=1$ (thick line) and $P_{\mathrm{dir}}=0$ (thin line). The dotted vertical line marks the propagation delay of the direct edge between the transmitter and the receiver. The parameter setting is listed in Table I.

the tails of the delay-power spectra in exhibit an exponential decay in both cases. This exponentially decaying power, which is not obtained by ad-hoc restrictions on the model parameters, is a result of recursive scattering in the graph.

To investigate the finer structure of the impulse response, it is necessary to have a better resolution in the delay domain. Therefore, we report in Fig. 4 the absolute value of an impulse respons obtained with $P_{\mathrm{dir}}=1$ using the parameter settings given in Table I, but with the frequency range extended such that $f_{\max}=10\,\mathrm{GHz}$. The impulse response in this case exhibits a specular-to-diffuse transition, i.e. the early part of the profile, dominated by specular contributions, is preceded

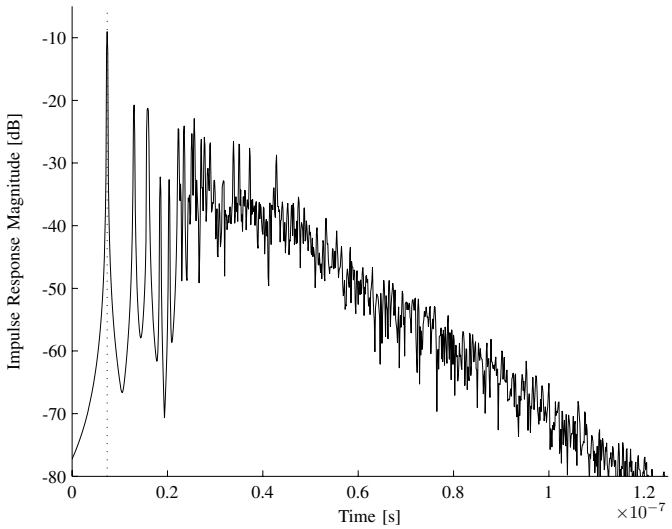

Fig. 4. Impulse response magnitude obtained from the model with $P_{\mathrm{dir}} = 1$. The parameter setting is as listed in Table I, but $f_{\max}$ has been set to 10 GHz.

by a diffuse tail. This shows that the model is able to jointly treat the specular and diffuse components of the impulse response.

V. Conclusions

A propagation model based on a stochastic propagation graph was proposed. The propagation model proposed [1] was extended to account for multi-input multi-output systems. Moreover, a closed form expression for the input-output relation was obtained.

A propagation graph is defined by a set of vertices (transmitters, receivers, and scatterers) and a set of edges (visibility between vertices). These parameters can be drawn randomly according to some joint probability density function.

Based on measurement results conventional models implement an exponentially decaying absolute impulse response and delay-power spectrum by various assumptions. These approaches, however, do not reflect the underlying physical mechanisms that lead to this decaying behaviour. It was shown by Monte Carlo simulations that assuming an inverse squared distance power decay, the proposed model yields the often observed exponentially decaying absolute impulse response and delay-power spectrum. This effect stems from the structure of the propagation graph and is not obtained by introducing any artificial assumptions.

The realisations of the impulse response obtained from the proposed model also exhibit a transition from specular contributions for low delays to a diffuse part at long delays as observed in measurements. The model can be easily extended to include dispersion in directions of departure and arrival.

Acknowledgement

This work was supported by Elektrobit and NEWCOM, the Network of Excellence in Communications.

References

[1] T. Pedersen and B. H. Fleury, "A realistic radio channel model based on stochastic propagation graphs," *Proceedings 5th MATHMOD Vienna – 5th Vienna Symposium on Mathematical Modelling*, vol. 1,2, p. 324, feb 2006.

[2] A. A. M. Saleh and R. A. Valenzuela, "A statistical model for indoor multipath propagation channel," *IEEE Journal on Selected Areas in Communications*, vol. SAC-5, no. 2, pp. 128–137, Feb. 1987.

[3] Q. H. Spencer, B. Jeffs, M. Jensen, and A. Swindlehurst, "Modeling the statistical time and angle of arrival characteristics of an indoor multipath channel," *IEEE Journal on Selected Areas in Communications*, vol. 18, no. 3, pp. 347–360, 2000.

[4] J. Laurila, A. F. Molisch, and E. Bonek, "Influence of the scatterer distribution on power delay profiles and azimuthal power spectra of mobile radio channels," *Proceedings of the IEEE 5th International Symposium on Spread Spectrum Techniques and Applications*, vol. 1, pp. 267–271, 1998.

[5] M. Franceschetti, "Stochastic rays pulse propagation," *IEEE Trans. Antennas and Propagation*, vol. 52, no. 10, pp. 2742–2752, Oct. 2004.

[6] J. Kunisch and J. Pamp, "Measurement results and modeling aspects for the UWB radio channel," *Ultra Wideband Systems and Technologies, 2002. Digest of Papers. 2002 IEEE Conference on*, pp. 19–24, May 2002.

[7] H. Kuttruff, *Room Acoustics*. London: Taylor & Francis, 2000.

[8] J. B. Andersen, J. Ødum Nielsen, G. Bauch, and M. Herdin, "The large office environment-measurement and modeling of the wideband radio channel," in *The 17th Annual IEEE International Symposium on Personal Indoor and Mobile Radio Communications*, 2006.

[9] R. Gerlach and V. Mellert, "Der Nachhallvorgang als Markoffsche Kette Theorie und erste experimentelle Überprüfung," *Acustica*, vol. 32, no. 4, pp. 211–227, apr 1975.

[10] R. Diestel, *Graph Theory*, electronic edition 2000 ed. Springer-Verlag, 2000. [Online]. Available: http://www.math.uni-hamburg.de/home/diestel/books/graph.theory/

[11] E. Bonek, M. Herdin, Werner, and H. Özcelik, "MIMO — study propagation first!" *Signal Processing and Information Technology, 2003. ISSPIT 2003. Proceedings of the 3rd IEEE International Symposium on*, pp. 150–153, Dec. 2003.

[12] G. Strang, *Introduction to Linear Algebra*, 3rd ed. Wellesley-Cambridge Press, 2003.